CSM-IXIM: A New Maize Simulation Model for DSSAT Version 4.5

J.I. Lizaso,* K.J. Boote, J.W. Jones, C.H. Porter, L. Echarte, M.E. Westgate, G. Sonohat

ABSTRACT

The CERES-Maize model is the most widely used maize (*Zea mays* L.) model and is a recognized reference for comparing new developments in maize growth, development, and yield simulation. The objective of this study was to present and evaluate CSM-IXIM, a new maize simulation model for DSSAT version 4.5. Code from CSM-CERES-Maize, the modular version of the model, was modified to include a number of model improvements. Model enhancements included the simulation of leaf area, C assimilation and partitioning, ear growth, kernel number, grain yield, and plant N acquisition and distribution. The addition of two genetic coefficients to simulate per-leaf foliar surface produced 32% smaller root mean square error (RMSE) values estimating leaf area index than did CSM-CERES. Grain yield and total shoot biomass were correctly simulated by both models. Carbon partitioning, however, showed differences. The CSM-IXIM model simulated leaf mass more accurately, reducing the CSM-CERES error by 44%, but overestimated stem mass, especially after stress, resulting in similar average RMSE values as CSM-CERES. Excessive N uptake after fertilization events as simulated by CSM-CERES was also corrected, reducing the error by 16%. The accuracy of N distribution to stems was improved by 68%. These improvements in CSM-IXIM provided a stable basis for more precise simulation of maize canopy growth and yield and a framework for continuing future model developments.

Since its release in 1986, CERES-Maize (Jones and Kiniry, 1986) has set a high standard for crop simulation models and has become the most widely used maize simulation model. The CERES-Maize model, together with other crop simulation models, was integrated into the Decision Support System for Agrotechnology Transfer (DSSAT). The first DSSAT release (version 2.1) was in 1989 (IBSNAT, 1989). Modularizing the model structure to facilitate information exchange among system components and model improvements led to the development of a uniform model structure within DSSAT, the Cropping System Model (CSM; Jones et al., 2003), which is now implemented for most crop models. The modular version of CERES-Maize, CSM-CERES-Maize, is currently distributed with DSSAT version 4.5 (Hoogenboom et al., 2010).

As our understanding of natural systems improves, and new applications, requirements, and expectations surface, model development has progressed toward more powerful and complex simulation systems. Legacy crop models, i.e., well-established simulators such as CSM-CERES-Maize, however, continue to provide a common benchmark for testing model improvements and for developing and evaluating new models. The new developments in maize modeling that we have developed were based on the legacy CSM-CERES-Maize model.

The simulation of plant leaf area, C assimilation, and N uptake and partitioning in CSM-CERES-Maize modules has received attention. Maize canopies can develop with considerable variation in leaf surface area (e.g., Elings, 2000; Birch et al., 2003). Even hybrids with the same final leaf number can show large differences in seasonal foliar surface area (Dwyer et al., 1992). The CSM-CERES-Maize model does not allow for variation in leaf area for a given leaf number, even though users can calibrate leaf number (PHINT) and total canopy leaf area. This may be why so many reports have presented inaccurate simulations of leaf area with this model (Carberry et al., 1989; Keating and Wafula, 1992; Lizaso and Ritchie, 1997; Ben Nouna et al., 2000; Lopez-Cedron et al., 2005). An alternative approach, such as that developed by Lizaso et al. (2003a), is needed in DSSAT to simulate maize leaf number and leaf area more accurately.

Despite the limitation for simulating leaf area, CSM-CERES-Maize estimates biomass accumulation and grain yield fairly accurately (Mastrorilli et al., 2003; Anapalli et al., 2005; Tojo-Soler et al., 2007), particularly in the absence of stress. It has been proposed that a more mechanistic approach to quantify photosynthesis and respiration would be superior to the radiation use efficiency currently used by CSM-CERES-Maize (Yang et al., 2004). In fact, photosynthesis and respiration have different responses to environmental conditions. For instance, maize leaf assimilation increases with temperature up to around 35°C and then decreases at higher temperatures (Oberhuber and Edwards, 1993; Naidu et al., 2003). The rate of dark respiration, however, continues to increase with temperature (Oberhuber

J. I. Lizaso, Dep. Producción Vegetal: Fitotecnia, Univ. Politécnica of Madrid, 28040 Madrid, Spain; K.J. Boote, Dep. of Agronomy, P.O. Box 110500, Univ. of Florida, Gainesville, FL 32611; J.W. Jones and C.H. Porter, Dep. of Agricultural and Biological Engineering, P.O. Box 110570, Univ. of Florida, Gainesville, FL 32611; L. Echarte, National Research Council of Argentina, EEA INTA Balcarce, Univ. Nacional de Mar del Plata, CC 276, 7620 Balcarce, Argentina; M.E. Westgate, Dep. of Agronomy, 2101 Agronomy Hall, Iowa State Univ., Ames, IA 50011; and G. Sonohat, ENITA Clermont, Site de Marmilhat, BP 35, 63370 Lempdes, France. Received 8 Oct. 2010.
*Corresponding author (jon.lizaso@upm.es).

Published in Agron. J. 103:766–779 (2011)
Published online 17 Mar 2011
doi:10.2134/agronj2010.0423

Abbreviations: CSM, Crop System Model; DSSAT, Decision Support System for Agrotechnology Transfer.

and Edwards, 1993). Also, maximum photosynthesis at low light intensity occurs at a much lower temperature than at saturating light intensity (Oberhuber and Edwards, 1993). Incorporating such mechanistic modules, however, without requiring additional weather inputs is important to ensure continued broad applications of the model (Lizaso et al., 2005a).

Crop N simulation by CSM-CERES-Maize has received limited attention. Some reports indicate that the model adequately simulates end-of-season crop N uptake (Pang et al., 1997; Asadi and Clemente, 2001). Nevertheless, detailed time course evaluations show an excessive simulated rate of N uptake immediately after a fertilization event. This hyperaccumulation of N by CSM-CERES-Maize suggests the need to refine N acquisition in new models.

The first objective of this work was to present and evaluate CSM-IXIM, a new maize simulation model that incorporates recent improvements in the simulation of leaf area, C assimilation and partitioning, ear growth, kernel number, grain yield, and plant N acquisition and distribution into DSSAT version 4.5. The second objective was to examine the stability of CSM-IXIM in response to changes in the parameters associated with the simulation of leaf area, shoot biomass, grain yield, and crop N.

MATERIALS AND METHODS

Ixim (pronounced *e-sheem*, [iʃim] according to the International Phonetic Alphabet), the Maya word for maize, is the name of our new maize model. Code from CSM-CERES-Maize version 4.5 was modified to include a number of improvements and new modules. For simplicity, the new maize simulation model, CSM-IXIM, will be referred to as IXIM, while CSM-CERES-Maize will be referred to as CERES.

Model Development

Leaf Area Simulation

Per-leaf foliar surface expansion and senescence was simulated following the procedures described by Lizaso et al. (2003a) with the following modifications. Leaf number (LFN), one of the required inputs of their model, is estimated early in the season using information available in the genetic coefficients. The value of LFN is recomputed later when leaf differentiation ends after the photoperiod-sensitive flower induction is completed:

$$\mathrm{LFN}=\frac{1.4\mathrm{P1}}{0.5\mathrm{PHINT}}+10.55-0.0216\mathrm{P1} \qquad [1]$$

where P1 is thermal time (degree days) from emergence to the end of the juvenile phase and PHINT is the phyllochron (degree days), the thermal time elapsed between the appearance of two consecutive leaf tips. Equation [1] generally assumes that the juvenile phase takes 25% and the flower induction phase takes 10% of the thermal time duration of the vegetative stage (emergence to flowering). This assumption fails for very short or very long season cultivars; thus the second part of Eq. [1] uses the coefficient P1 to adjust LFN for those cultivars. Equation [1] also assumes that five leaves are differentiated at emergence (Jones and Kiniry, 1986). After the photoperiod-sensitive flower induction phase is completed, LFN is recalculated based on the number of differentiated leaves, replacing the value obtained with Eq. [1] for the remainder of the growing season. In this way, only two new genetic coefficients are required, as described below.

Additional changes included the effects of temperature and stress on leaf area simulation. The temperature effect on leaf expansion (Tf) was derived from Salah and Tardieu (1996):

$$\begin{aligned}\mathrm{Tf}&=1.15\left\{1-\exp\left[-0.2(\mathrm{TM}-9.8)\right]\right\} && \mathrm{TM}\le 32^{\circ}\mathrm{C}\\ \mathrm{Tf}&=4.8-0.118\mathrm{TM} && \mathrm{TM}>32^{\circ}\mathrm{C}\end{aligned} \qquad [2]$$

where TM is the daily mean air temperature. The value of Tf is constrained between zero and one and multiplied by the potential leaf expansion rate. Equation [2] assumes a base temperature of 9.8°C and that leaf expansion is at its potential maximum between mean air temperatures of 20 and 32°C. The model also calculates an expansion reduction factor based on the most limiting stress due to soil water deficit, aeration, N, and P.

Under water stress, leaf rolling reduces the effective light capture of maize canopies. The effect of leaf rolling on photosynthetically active radiation (PAR) absorption is estimated by calculating an hourly fraction of effective light-capturing leaf area (Fla):

$$\mathrm{Fla}=\frac{\mathrm{SF_W}+(h-14)^2}{\mathrm{Amp}} \qquad [3]$$

where

$$\mathrm{Amp}=\left\{25+(100-25)\exp\left[-3.5(1-\mathrm{AT})\right]\right\}\times\left(5-4\mathrm{SF_w}\right) \qquad [4]$$

and SF_W is the zero-to-one most-limiting water stress factor (TURFAC) as used in CERES, h is the hour of the day, and Amp is an amplitude parameter integrating the interaction between water stress and atmospheric demand on leaf rolling. Because IXIM was developed to run with minimum weather inputs, no information is available to estimate atmospheric demand and thus a surrogate variable (AT) is used, which is the fraction of radiation transmitted through the atmosphere calculated hourly from canopy-incident and extraterrestrial solar radiation. Equations [3] and [4] were derived from measurements of light interception and leaf rolling by Carlesso (1993). The value of Fla is constrained between zero and one; Fla equals one when soil water is not limiting ($SF_W = 1$) and equals SF_W at 1400 h when soil water becomes limiting for expansion growth (Fig. 1). Under water stress, hourly values of Fla reduce per-leaf light capture.

Plant Growth Simulation

The code for simulation of dry matter growth and partitioning in CERES was completely replaced in IXIM. New modules computing per-leaf light absorption, instantaneous leaf CO_2 assimilation, daily canopy gross assimilation, and canopy respiration replace the PAR use efficiency approach in CERES.

Light capture, photosynthesis, and respiration follow the procedures detailed and tested by Lizaso et al. (2005a,b) and briefly summarized next. Daily solar radiation input is converted to PAR (Lizaso et al., 2003b) and then hourly averages of instantaneous photosynthetic photon flux density (PPFD, μmol quanta m^{-2} leaf s^{-1}) are computed with a sinusoidal function (Spitters et al., 1986). Fluxes of direct and diffuse light in the canopy are calculated (modified from Spitters et al., 1986) to estimate the light absorbed by sunlit and shaded portions of each leaf (Goudriaan, 1977). A hedgerow calculation (Boote and Pickering, 1994) hourly adjusts the fraction

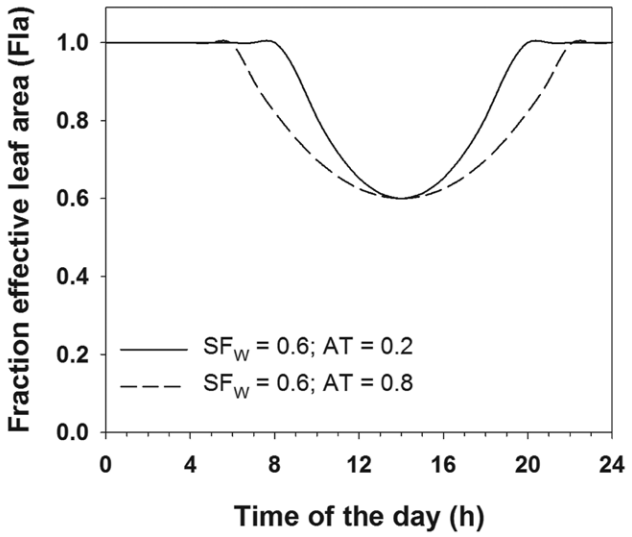

Fig. 1. Effect of water stress (SF_W) and atmospheric transmission of radiation (AT) on the fraction of effective light-absorbing leaf area for a cloudy day (AT = 0.2) and a clear day (AT = 0.8). The SF_W is the daily most-limiting water stress factor (TURFAC) controlling the simulation of cell expansion processes; AT is the hourly ratio of canopy incident solar radiation to extraterrestrial solar radiation.

of incoming PPFD being effectively captured by incomplete canopies. Every hour, instantaneous C gross assimilation (μmol CO_2 m^{-2} leaf s^{-1}) by each green leaf is calculated using a nonrectangular hyperbola function (Thornley and Johnson, 1990) of absorbed PPFD with a maximum assimilation rate of 57 μmol m^{-2} s^{-1} at 30°C (Choudhury, 2001). The effects of temperature and leaf age on leaf assimilation are estimated modifying the curve parameters. Changes in hyperbola parameters with temperature are calculated according to Oberhuber and Edwards (1993). Changes in parameters with the relative age of individual leaves are modified from Stirling et al. (1994). Canopy gross assimilation is calculated by daily integration of the 1-h contributions of successive vertical leaf classes of sunlit and shaded leaf area. Canopy respiration accounts for maintenance respiration (Wilkerson et al., 1983) and growth respiration for tissue synthesis (Penning de Vries and van Laar, 1982). More details were provided by Lizaso et al. (2005a).

A new growth partitioning approach (Fig. 2a) allocates biomass to individual leaf blades and ear structures before flowering. In the model, only leaf blades are considered leaf tissue and stem tissue includes leaf sheaths and tassel. Before tassel initiation, one-third of the daily plant biomass accumulation is allocated to root tissue (Grant, 1989). This proportion decreases linearly until

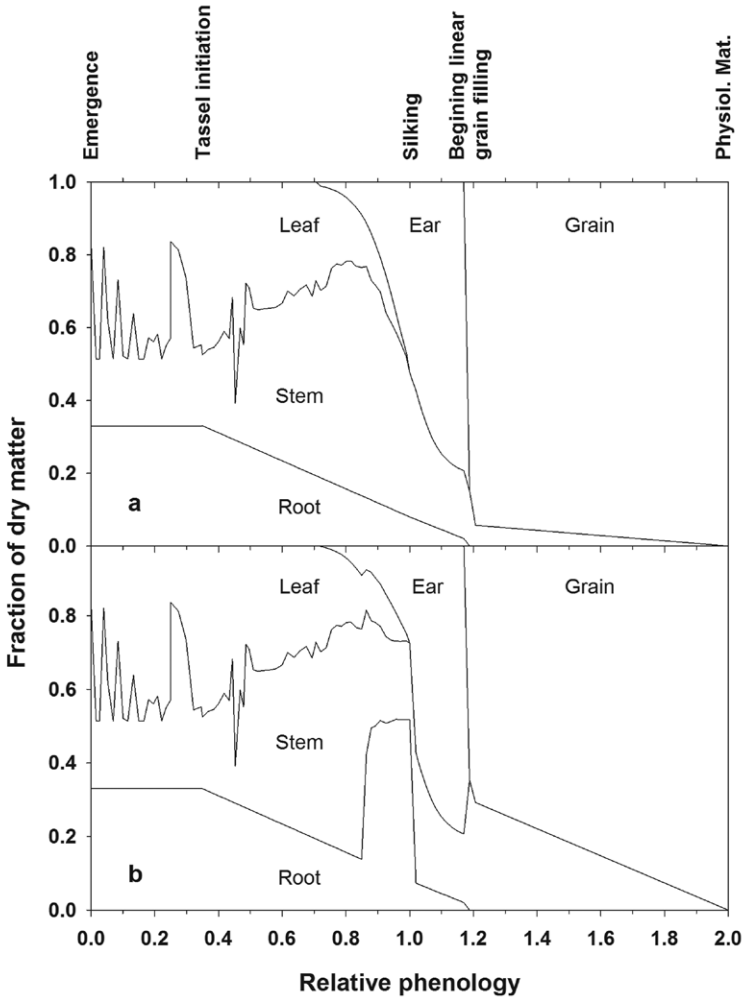

Fig. 2. Example of the CSM-IXIM model seasonal dry mass partitioning to tissues across a relative phenological scale (zero = emergence, 1 = silking, 2 = physiological maturity) for (a) no stress and (b) severe presilking water stress conditions. Well-irrigated, fertilized and rainfed, low-N treatments of the DSSAT distributed UFGA8201 experiment were used to simulate the no-stress and severe-stress conditions.

the beginning of the linear grain-filling phase when root growth stops and grain becomes the priority sink for assimilates.

Leaves and stem share the available dry mass until ear growth begins. Assimilate demand for the growth of each leaf is estimated and the remaining dry mass is allocated to stems. The biomass requirement for new leaf tissue is calculated from the leaf expansion rate ($cm^2\ d^{-1}$) divided by the specific leaf area (SLA, $cm^2\ g^{-1}$). Daily estimation of SLA for each leaf dynamically accounts for the effects of light intensity, mean air temperature, and leaf position within the canopy. This explains the variations in C partitioning between leaf and stem depicted in Fig. 2. A relative effect of daily light intensity (SL_L) on SLA is estimated from the measurements of Warrington and Norton (1991):

$$SL_L = 0.44 + (1.9 - 0.46)\exp(-0.165\,PAR) \quad [5]$$

where PAR is the daily photosynthetically active radiation ($MJ\ m^{-2}\ d^{-1}$) estimated from the input solar radiation (Lizaso et al., 2003b). Lower leaves in a maize canopy are thinner than upper leaves. Next, the effect of leaf position (SLi, $cm^2\ g^{-1}$) is calculated:

$$SLi = SL_L\left[SLAmn + (SLAmx - SLAmn) \times \exp\left(-S\frac{LFi}{LFN}\right)\right] \quad [6]$$

where SLAmn and SLAmx (270 and 750 $cm^2\ g^{-1}$, respectively) are parameters controlling the lower and upper bounds of SLA fitted to published data (Thiagarajah and Hunt, 1982; Tanaka and Yamaguchi, 1972), LFi is the leaf position relative to the total leaf number (LFN), and S is computed from the plant population density (PD, plant m^{-2}):

$$S = 9.0 - 0.275\,PD \quad [7]$$

Finally, a relative correction (SL_T) is calculated when the mean air temperature (TM, °C) is <32°C according to Thiagarajah and Hunt (1982):

$$SL_T = SLi\left(Ti + Ts\frac{LFi}{LFN}\right)$$
$$Ti = 0.0003TM^2 - 0.0095TM + 1.0696$$
$$Ts = 0.0222TM\text{-}0.8313 \quad [8]$$

If daily C assimilation limits shoot growth, leaf dry matter growth is constrained according to the available C supply. Subsequently, SLA is recalculated by dividing the updated leaf surface values by the leaf weight.

Under soil water and N stress conditions (Fig. 2b), partitioning of daily assimilates is modified, giving roots a greater proportion at the expense of the shoots. Figure 2b shows an increase in root biomass partitioning in response to water stress before flowering (relative phenology 0.85–1.00). The reduction in assimilates partitioned to the shoot, based on a similar concept developed by Penning de Vries and van Laar (1982), is controlled by

$$FS = 0.46 + 0.72\exp[-2.83(1 - SF)] \quad [9]$$

where FS is the fraction of shoot assimilate reduction due to stress, and SF is the most limiting of water or N stress factors (from 0.0 to 1.0). The FS parameter assumes that partitioning to shoots could be reduced by up to 50% under extreme stress conditions. With no stress, FS is constrained to one.

Grain Yield Simulation

Ear growth starts 250 growing degree days (GDD) before silking (Otegui and Bonhomme, 1998) and follows a sigmoidal function similar to the one previously reported for sweet corn (Lizaso et al., 2007):

$$F_E = \frac{P_E PGR}{1 + \exp[-0.02(tt - 225)]} \quad [10]$$

where F_E is the fraction of daily dry mass partitioned to the ear, PGR is the daily plant growth rate ($g\ plant^{-1}\ d^{-1}$), P_E is an ear partition parameter, and tt is the thermal time after the onset of ear growth (°C d). Equation [10] simulates a reduction of assimilates partitioned to the ear under conditions restrictive to plant growth (Pagano and Maddonni, 2007). It also allows for genetic variation in ear partitioning (P_E) as documented for modern vs. older genotypes (Echarte et al., 2004). Ear tissues (ovaries first, kernels after fertilization, cob, rachis, husks) continue to grow indistinctly until the end of the lag phase (170 GDD after 50% silking). Of those tissues, only seeds grow during the grain-filling phase. Under favorable conditions, assimilates in excess of grain sink capacity are allocated into stems.

Kernel number per plant is calculated as a curvilinear function of the average daily shoot growth rate (SGR, $g\ plant^{-1}\ d^{-1}$) computed across the same thermal time window used for ear growth:

$$KN1 = G2[1 - \exp(-0.347SGR)]$$
$$KN2 = 1.8G2\{1 - \exp[-0.895(SGR\text{-}3.0)]\} \quad [11]$$

where G2 is the cultivar-specific potential number of seeds on the uppermost ear, a model genetic coefficient. This definition is different from the definition of G2 in CERES, where it is the potential number of seeds per plant. Equation [11] simulates kernel number in the uppermost ear (KN1), and in a second ear (KN2) if SGR is large (i.e., >3.6 $g\ plant^{-1}\ d^{-1}$), which frequently occurs at low population densities (Fig. 3). Data to fit Eq. [11] were collected in Ames, IA, in 2000. Hybrid Asgrow 740 was sown at 1, 4, 8, and 16 plants m^{-2} and fertilized at 56, 168, or 336 kg N ha^{-1}. The crop grew throughout the season under near-optimum conditions, and kernel numbers in apical and subapical ears were determined shortly after physiological maturity. Shoot growth rates were determined for individual plants using previously calculated correlations between morphometric measurements (stem diameter, ear diameter, and ear length) and plant dry matter (Andrade et al., 1999). The IXIM model also simulates barrenness (<1 ear $plant^{-1}$) and prolificacy (>1 ear $plant^{-1}$) as a function of shoot growth rate:

$$EAR1 = 1 - \exp(-SGR)$$
$$EAR2 = 2\{1 - \exp[-0.875(SGR\text{-}2.8)]\} \quad [12]$$

Equations [11] and [12] indicate a threshold shoot growth rate for a second kernel-bearing ear of 3.6 $g\ plant^{-1}\ d^{-1}$ during the critical period for kernel set.

Plant Nitrogen Simulation

The CERES model simulates three compartments of plant N: shoot, root, and grain. The IXIM model, in addition to root and grain N, further partitions shoot N into leaves, stem, and ear components. Critical N concentrations (NC, %), those

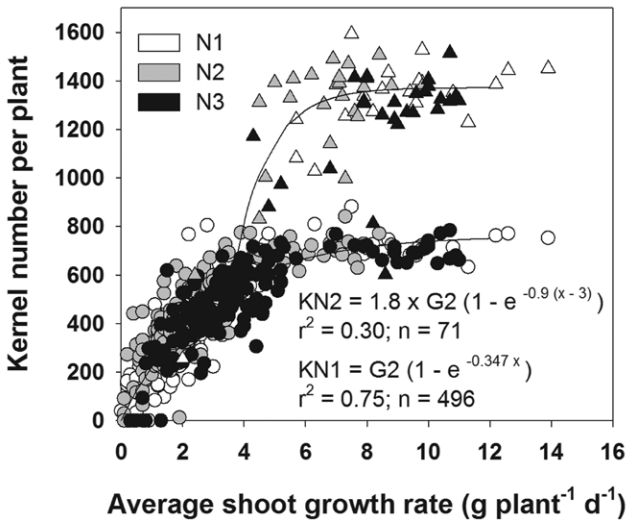

Fig. 3. Relationship of kernel number per plant for the topmost ear (KN1) and the second ear (KN2) for the Asgrow 740 hybrid grown at three N rates (56 [N1], 168 [N2], and 336 [N3] kg N ha^{-1}) in Ames, IA; G2 is the potential number of seeds in the uppermost ear.

tissue N levels below which growth is reduced (Jones, 1983; Jones and Kiniry, 1986), for leaves, stem, and ear are:

$$\begin{aligned} NC_L &= 5.06\exp(-0.11\,RPH) \\ NC_S &= 4.8\,RPH^{-1.15} \\ NC_E &= 4 - 0.0086\,tt \end{aligned} \quad [13]$$

Leaf critical N concentration (NC_L) is calculated after Lindquist and Mortensen (1999), where RPH is a 0 to 10 relative scale for phenological development used also by CERES, with a value of 4.5 at silking and 10.0 at physiological maturity. Critical N concentration in stems (NC_S) is maintained at 4% during the juvenile phase and decreases linearly down to 3% during the flower induction phase. After the tassel is initiated, NC_S is calculated using Eq. [13]. The critical N concentration for the ear (NC_E) is calculated according to Eq. [13] during the thermal time (tt, °C d) period for rapid ear growth (250°C d before silking through 100°C d after silking). After ear growth is complete, NC_E is maintained at 1%. Values computed with Eq. [13] are divided by 100 to calculate corresponding fractions.

Plant N acquisition follows similar assumptions as in CERES, with an additional constraint on maximum daily uptake. Maximum daily N uptake (Nmax, g plant^{-1} d^{-1}) is limited by a curvilinear function dependent on the daily plant growth rate (PGR, g plant^{-1} d^{-1}):

$$Nmax = Nx\left[1 - \exp(-0.8\,PGR)\right] \quad [14]$$

where Nx is the maximum rate of N uptake (0.06 g plant^{-1} d^{-1}) observed under unrestrictive growing conditions. This constraint is an attempt to account for the energy cost of N uptake, reduction, and assimilation.

Additional Model Inputs

The simulation of cultivar-specific leaf area in IXIM requires two coefficients in addition to those needed for CERES. The new inputs control the size of the largest leaf and maximum leaf longevity and should be determined experimentally under unstressed conditions:

- AX: one-side surface area of the largest leaf (cm^2 leaf^{-1});
- LX: longevity of the most long-lived leaf (degree days), defined as the thermal time elapsed between 50% leaf expansion and 50% senescence.

When the new inputs are not available in the cultivar file, default values are calculated. The value of AX is estimated from the leaf number after Birch et al. (1998):

$$AX = 1000\exp(-1.17 + 0.047\,LFN) \quad [15]$$

and LX is estimated from AX following the regression analysis of calibrated values ($r^2 = 0.989$; $P < 0.001$; $n = 8$):

$$LX = 1.114\,AX \quad [16]$$

A summary of variables used by IXIM is presented in Table 1.

Model Evaluation

Model Evaluation Data

Data distributed with DSSAT version 4.5 was used for model testing. The CERES and IXIM outputs were compared using the default Simulation Options in DSSAT: observed atmospheric CO_2 concentration (Keeling et al., 2001), evapotranspiration by the Priestley–Taylor method (Priestley and Taylor, 1972), soil evaporation by the Suleiman–Ritchie method (Suleiman and Ritchie, 2003), and soil organic matter by the Godwin–Jones method (Godwin and Jones, 1991).

The simulation of per-leaf foliar surface in IXIM was tested with data collected by Sonohat (1997) in Grignon, France. Soil information for the experimental site was obtained from Gabrielle et al. (1995). Maize, hybrid Dea, was sown in 1994 and 1995 following a Nelder design (Nelder, 1962), yielding plant population densities ranging from 5 to 25 plants m^{-2}. The leaf area of individual leaves was evaluated as the product of length times the maximum width times a coefficient (0.75) determined independently by regression analysis for the cultivar used. Genetic coefficients were calibrated using the information collected in 1994 at 5 plants m^{-2}.

Testing Model Accuracy

Two statistical indices were used to compare the observed and model-simulated values. The RMSE was calculated as

$$RMSE = \left[\frac{1}{n}\sum_{i=1}^{n}(S_i - O_i)^2\right]^{0.5} \quad [17]$$

where S_i and O_i are a corresponding pair of simulated and measured values, respectively, and n is the number of observations included in the evaluation. The parameter d or Willmott's index of agreement (Willmott, 1982) was calculated as

$$d = 1 - \left[\frac{\sum_{i=1}^{n}(S_i - O_i)^2}{\sum_{i=1}^{n}\left(\left|S_i'\right| + \left|O_i'\right|\right)^2}\right] \quad [18]$$

where $S_i' = S_i - \bar{O}$ and $O_i' = O_i - \bar{O}$. Parameter d lies within the range zero to one, with higher values indicating more accurate simulations.

Table 1. Definition, units, and file available of variables used by IXIM.

Variable	Definition	Unit	File
Amp	coefficient controlling the daily time amplitude of leaf rolling	–	internal
AT	fraction of solar radiation transmitted through the atmosphere	–	internal
AX	one-side surface area of the largest leaf	cm^2 $leaf^{-1}$	cultivar
EAR1	average number of ears per plant in the uppermost position	ear $plant^{-1}$	internal
EAR2	average number of ears per plant in uppermost and second positions	ear $plant^{-1}$	internal
F_E	fraction of daily assimilates partitioned to the ear	–	internal
Fla	hourly fraction of effective light-capturing leaf area due to leaf rolling	–	internal
FS	relative reduction of shoot assimilates partitioning due to water and N stress	–	internal
G2	potential number of seeds in uppermost ear	seed ear^{-1}	cultivar
h	hour of the day	h	internal
KN1	kernel number in the uppermost ear	seed ear^{-1}	internal
KN2	kernel number in the second ear	seed ear^{-1}	internal
LFi	leaf position in a maize canopy determined acropetally	–	internal
LFN	total number of leaves	–	internal
LX	longevity of the most long-lived leaf in thermal time	°C d	cultivar
NC_E	ear critical N concentration	fraction	internal
NC_L	leaf critical N concentration	fraction	internal
NC_S	stem critical N concentration	fraction	internal
Nmax	daily maximum N uptake	g $plant^{-1}$ d^{-1}	internal
Nx	maximum rate of n uptake under non-restrictive conditions	g $plant^{-1}$ d^{-1}	internal
PAR	photosynthetically active radiation	MJ m^{-2} s^{-1}	internal
PD	plant population density	plant m^{-2}	experiment
P_E	parameter controlling the fraction of assimilates partitioned to the ear		ecotype
PGR	daily plant (shoot + root) growth rate	g $plant^{-1}$ d^{-1}	internal
P_S	parameter controlling the fraction of assimilates partitioned to the stem		ecotype
RPH	relative scale (0–10) for phenological development	–	internal
S	relative effect of plant population density on specific leaf area	–	internal
SF	most limiting of water or N stress coefficients	–	internal
SF_W	relative water stress coefficient	–	internal
SGR	daily shoot growth rate	g $plant^{-1}$ d^{-1}	internal
SLA	specific leaf area	cm^2 g^{-1}	internal
SLAmn	lower bound of specific leaf area	cm^2 g^{-1}	species
SLAmx	upper bound of specific leaf area	cm^2 g^{-1}	species
SL_i	effect of canopy leaf position on specific leaf area	cm^2 g^{-1}	internal
SL_L	relative effect of daily light intensity on specific leaf area	–	internal
SL_T	relative effect of daily mean air temperature on specific leaf area	–	internal
Tf	relative effect of temperature on leaf expansion	–	internal
Ti	parameter used to calculate SL_T	–	internal
TM	daily mean air temperature	°C	internal
Ts	parameter used to calculate SL_T	–	internal
tt	thermal time (8°C base temperature) after the onset of ear growth	°C d	internal

Sensitivity Analysis

Model stability was examined under near-optimum growing conditions and under water and N stress conditions. The DSSAT-distributed experimental data set UFGA82 was used as the base case with two treatments investigated: irrigated with high N and rainfed with low N. The stress treatment received 5% of the seasonal irrigation and 29% of the N fertilization of the no-stress treatment, thus growing under stress most of the season. In each model run, a single coefficient was changed within ±30% of its original value and the effects on associated model outputs were recorded. In total, four related coefficients were changed for each model output examined. Four model outputs were monitored: leaf area index (LAI) at silking, biomass at maturity, grain yield, and N content in shoots at maturity. Relative changes in model outputs were plotted against relative changes in input coefficients for stress and no-stress conditions.

RESULTS AND DISCUSSION

The main components of IXIM were evaluated by comparing the simulations obtained with CERES and with IXIM against measured values. Evaluated components included per-leaf surface area, LAI, aboveground biomass and partitioning among organs, shoot N content, and leaf and stem N concentrations. Per-leaf surface area was tested only for IXIM. No change in phenology was introduced in IXIM relative to CERES.

Leaf Area

The simulated leaf surface area (Fig. 4) was remarkably accurate for different years and population densities, with Willmott's *d* values >0.993 and RMSE values of 35 cm^2 $leaf^{-1}$ or less, which is within 6% of the corresponding largest leaf (Table 2). The simulation of the whole canopy leaf area (Fig. 5) also yielded good results, with *d* values ranging within 0.604 to 0.977 for CERES and within 0.927 to 0.990 for IXIM. Under stressful conditions,

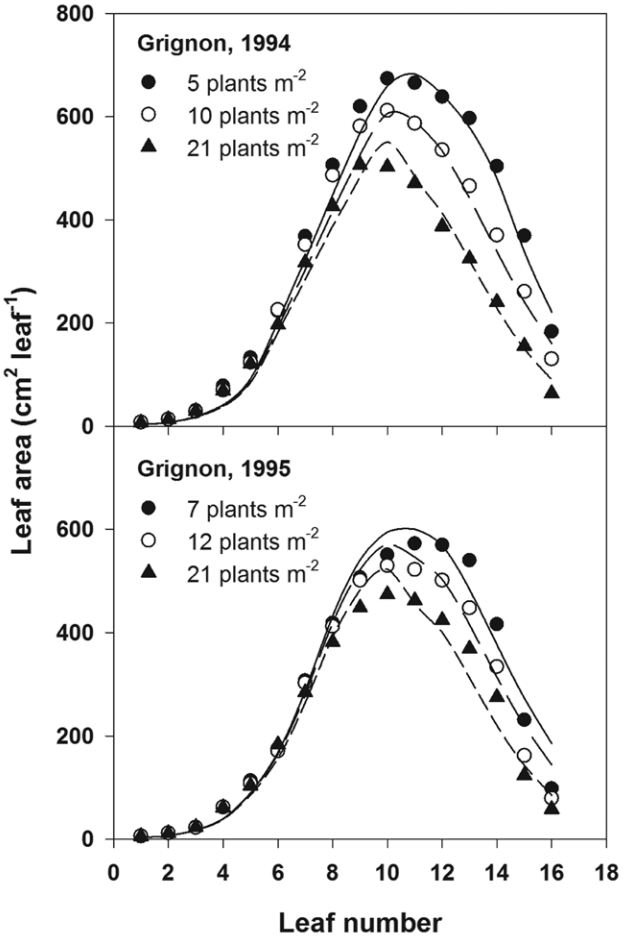

Fig. 4. Time course for simulated and observed leaf area of individual leaf blades at full expansion of the DEA hybrid grown in Grignon, France, at three population densities during 1994 (top) and 1995 (bottom).

both models generated less accurate simulations of LAI, but IXIM performed better in nearly all cases, with an average improvement of 23% in *d* (Table 2). The CERES model did not simulate peak leaf area at flowering correctly for the H610 hybrid in Hawaii. Similar results were reported previously by Lizaso et al. (2003a) using different data in an earlier version of DSSAT.

Biomass Accumulation and Partitioning

Seasonal progressions of biomass accumulation simulated by IXIM and CERES are shown in Fig. 6 for various experiments and treatments. The IXIM and CERES models closely simulated total aboveground biomass and grain yield, particularly under favorable growing conditions (Fig. 6, left panels). Values of RMSE for CERES were within the range of 167 to 2229 kg ha^{-1}, and 426 to 1324 kg ha^{-1} for IXIM. Corresponding ranges for Willmott's *d* statistic were 0.946 to 0.997 for CERES and 0.721 to 0.997 for IXIM.

The lowest *d* value for IXIM was obtained for simulations of grain yield in the Florida 2001 experiment, in which no N was applied. In this treatment, N supply depended largely on mineralization of residues from the previous crop (*Arachis hypogaea* L.). Both CERES and IXIM calculate a pool of N available for translocation to the grain, which may constrain kernel numbers and grain yield under limited N supply. As discussed below, CERES overestimates N uptake when abundant soil N is

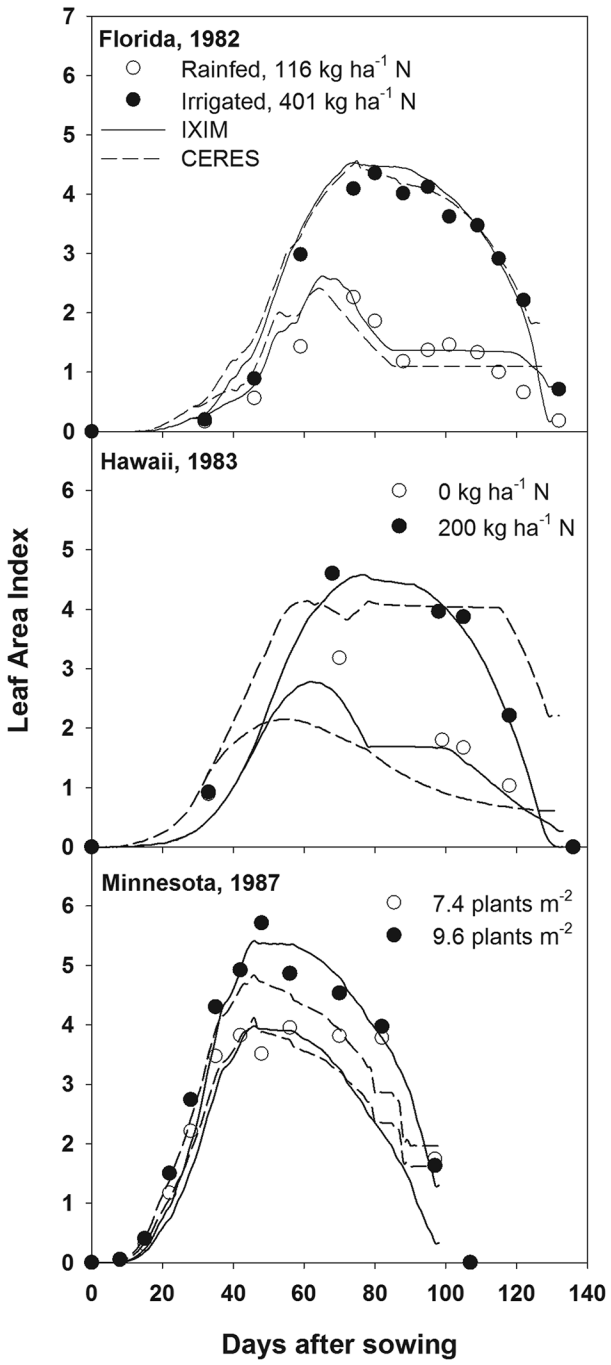

Fig. 5. Measured (symbols) and simulated (lines) leaf area index of maize experiments conducted in Florida, Hawaii, and Minnesota. Simulations were performed with CSM-CERES-Maize (dashed lines) and with CSM-IXIM (continuous lines).

provided through fertilization. In this case, CERES calculated a 40% larger N pool at the beginning of the linear grain filling. The smaller N pool simulated by IXIM resulted in 57% fewer kernel numbers than measured for this treatment, compared with 39% fewer kernel numbers simulated by CERES (data not shown).

The growth of stems and leaves is shown in Fig. 6 (right panels; note the change in scale with respect to the left panels). The CERES model tended to overestimate leaf biomass and underestimate stem biomass. The IXIM model, on the other hand, simulated leaf mass more accurately, although the simulated stem biomass was greater than the measured values

Table 2. Root mean square error (RMSE) and Willmott's *d* statistic (Willmott, 1982) calculated with measured time-series values and corresponding simulations obtained with two maize simulation models, CSM-CERES-Maize (CERES) and CSM-IXIM (IXIM).

				RMSE		*d*	
Variable	**Exp.†**	**Treatment**	**Organ**	**CERES**	**IXIM**	**CERES**	**IXIM**
Leaf area	GR94	5 plants m^{-2}	leaf		31.035		0.996
		10 plants m^{-2}	leaf		32.474		0.994
		21 plants m^{-2}	leaf		25.046		0.995
	GR95	7 plants m^{-2}	leaf		35.057		0.993
		12 plants m^{-2}	leaf		28.852		0.995
		21 plants m^{-2}	leaf		28.979		0.993
Leaf area index	FL82	rainfed, 116 kg N ha^{-1}	leaf	0.388	0.287	0.808	0.927
		irrigated, 401 kg N ha^{-1}	leaf	0.394	0.267	0.975	0.990
	HI83	Hybrid H610, 0 kg N ha^{-1}	leaf	0.839	0.384	0.604	0.938
		Hybrid H610, 200 kg N ha^{-1}	leaf	0.771	0.275	0.902	0.990
	MN87	7.4 plants m^{-2}	leaf	0.506	0.738	0.966	0.936
		9.6 plants m^{-2}	leaf	0.537	0.396	0.977	0.990
Biomass	FL82	rainfed, 116 kg N ha^{-1}	leaf	1060.539	553.047	0.459	0.671
			stem	214.373	1124.865	0.983	0.753
			grain	290.759	426.039	0.961	0.936
			shoot	867.840	1163.169	0.957	0.944
		irrigated, 401 kg N ha^{-1}	leaf	1054.543	235.521	0.802	0.982
			stem	1781.505	626.113	0.856	0.986
			grain	539.500	555.631	0.995	0.995
			shoot	831.603	850.350	0.997	0.997
	IA99	56 kg N ha^{-1}	leaf	798.442	712.070	0.907	0.940
			stem	1171.738	1125.951	0.850	0.881
			ear	1155.416	1526.327	0.931	0.875
			shoot	2229.099	881.693	0.946	0.993
		224 kg N ha^{-1}	leaf	693.975	578.500	0.950	0.970
			stem	1352.287	916.625	0.835	0.926
			ear	822.106	875.232	0.993	0.992
			shoot	1647.651	1031.520	0.989	0.996
	FL01	0 kg N ha^{-1}	leaf	635.349	189.672	0.642	0.929
			stem	135.621	1104.025	0.993	0.773
			ear	396.496	1182.572	0.970	0.736
			grain	166.727	829.721	0.987	0.721
			shoot	771.334	766.115	0.973	0.974
		240 kg N ha^{-1}	leaf	584.813	432.794	0.856	0.873
			stem	1278.308	951.739	0.850	0.911
			ear	734.986	423.623	0.993	0.997
			grain	305.610	814.427	0.993	0.914
			shoot	780.069	1323.671	0.996	0.988
Plant N	FL82	rainfed, 116 kg N ha^{-1}	shoot	32.642	34.107	0.632	0.695
			leaf %	0.886	1.126	0.479	0.223
			stem %	0.965	0.278	0.638	0.944
		irrigated, 401 kg N ha^{-1}	shoot	21.739	20.547	0.978	0.982
			leaf %	1.081	0.635	0.614	0.780
			stem %	0.947	0.362	0.817	0.966
	IA99	56 kg N ha^{-1}	shoot	16.525	9.566	0.705	0.858
			leaf %	0.347	0.831	0.968	0.851
			stem %	0.541	0.244	0.724	0.853
		224 kg N ha^{-1}	shoot	28.476	28.739	0.901	0.930
			leaf %	0.332	0.733	0.971	0.884
			stem %	1.450	0.285	0.433	0.844
	FL01	0 kg N ha^{-1}	shoot	10.233	9.587	0.802	0.809
			leaf %	0.469	0.652	0.914	0.843
			stem %	0.521	0.127	0.926	0.995
		240 kg N ha^{-1}	shoot	18.954	6.105	0.967	0.997
			leaf %	0.904	0.656	0.745	0.847
			stem %	0.940	0.401	0.836	0.957

† GR***nn***, Grignon, France, year; FL***nn***, Florida, year; HI***nn***, Hawaii, year; MN***nn***, Minnesota, year; IA***nn***, Iowa, year.

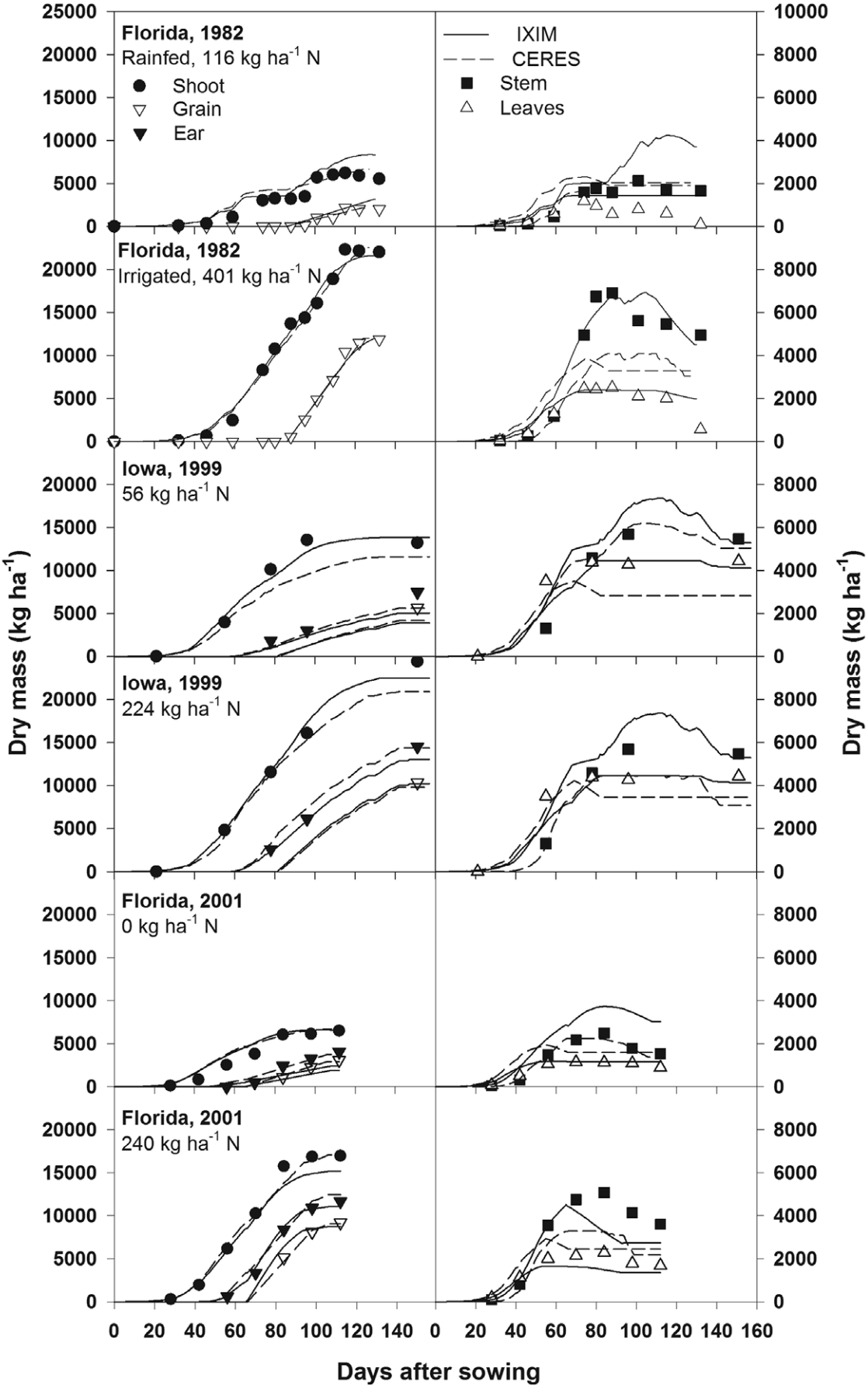

Fig. 6. Measured (symbols) and simulated (lines) maize dry mass accumulation for shoots, ears, and grain (left) and for stems and leaves (right). Note the difference in scale between the two panels. Simulations were performed with CSM-CERES-Maize (dashed lines) and with CSM-IXIM (continuous lines).

when plants were grown under significant water or N stress conditions. The IXIM model includes an explicit algorithm to increase partitioning to roots (Eq. [9]) under water or N stress. Under extreme stress, Eq. [9] increases partitioning to roots up to 50% C at the expense of shoots. Simulation of leaf rolling also reduces the amount of light capture during water stress (Eq. [3]), decreasing plant growth. A more detailed analysis of stem dry mass in the Florida 1982 rainfed treatment indicated that simulated values greatly overestimated the observed values after rainfall relieved a long (22-d) period of strong water stress. The IXIM model accurately simulated the remaining leaf area (Fig. 5) but recovered C assimilation to nonlimiting rates after stress. Growth measurements indicated, however, that C assimilation recovery was delayed or seriously impaired. The failure to recover was probably due to nonstomatal inhibition of photosynthesis, which currently is not considered. Future improvements of the photosynthesis module of IXIM should include these well-known effects of severe water and temperature stress.

Crop Nitrogen Simulation

Accurate simulation of plant N content depends on the correct calculation of biomass and N concentrations in tissues. Crop N accumulation during the growing season is shown in Fig. 7. Nitrogen uptake simulated by CERES was too rapid after fertilization. This excessive uptake was mostly corrected in IXIM (Eq. [14]). Simulation improvements were on the order of 0.4% up to >15% according to Willmott's *d* (Table 2). In the 1982 Florida experiment stress treatment, IXIM overestimated shoot N content at the end of the season, which was probably due to the additional partitioning of C for stem growth discussed above.

The CERES model simulates shoot N concentration based on the critical and minimum shoot and root N concentrations of Jones (1983). For output purposes, the CERES model partitions daily shoot N to stem and leaves based on the biomass of each tissue, resulting in identical N concentrations. Ear N is not simulated separately. The IXIM model calculates N pools for leaf, stem, and ear based on separate critical N concentrations (Eq. [13]). Figure 8 shows the simulated leaf and stem N concentrations by CERES and IXIM. Stem N concentrations simulated by IXIM were always close to measured values, with *d* values ranging between 0.844 and 0.995, compared with 0.433 to 0.926 for CERES. To correctly interpret the N concentration in leaves, it must be noted that leaf N was measured in green leaves while simulated leaf N takes into account both green and senesced leaves. Also, at this time, IXIM does not calculate the N concentration in individual leaves but rather on leaf mass of the whole canopy. Additional improvement of leaf N concentration may result from the simulation of N dynamics of individual leaves, including N remobilization from old leaves to other developing tissues.

Sensitivity Analysis

The stability of IXIM was examined by systematically varying parameters associated with the simulation of leaf area, biomass, yield, and aboveground crop N (Fig. 9). Only one parameter was changed at a time, within the range ±30% from initial values. Model output sensitivity was evaluated under near-optimum growing conditions and under water and N stress.

The simulation of LAI at silking showed a dramatic response to variation in the new genetic coefficients AX (surface area

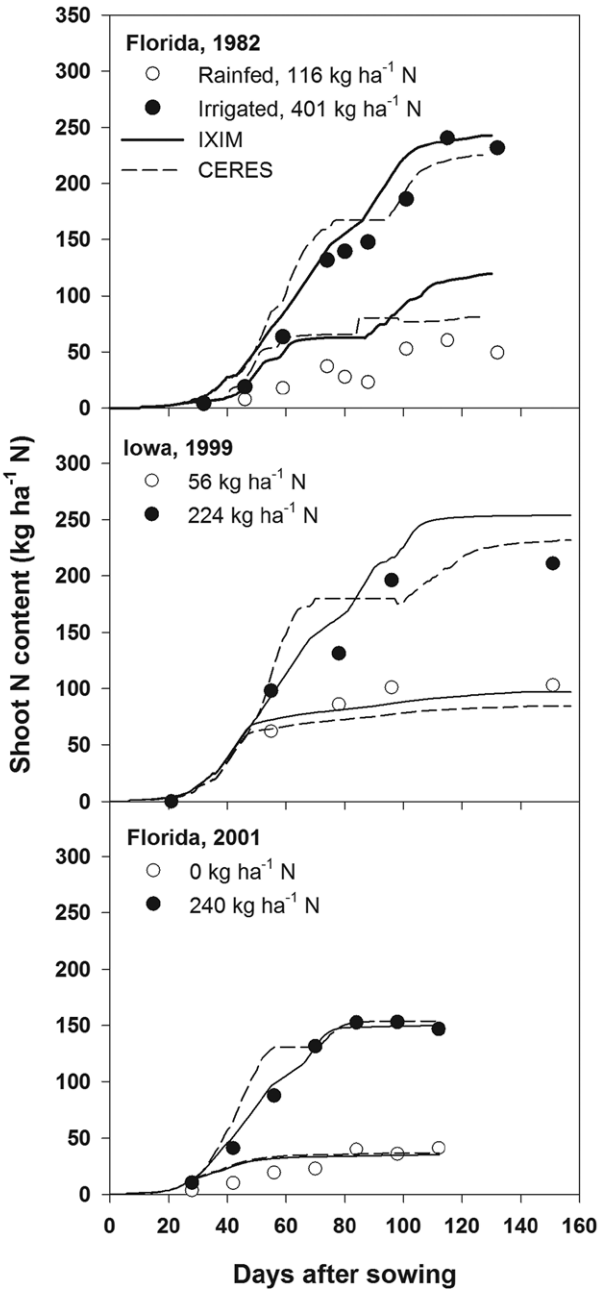

Fig. 7. Measured (symbols) and simulated (lines) N contents in shoots of maize experiments conducted in Florida and Iowa. Simulations were performed with CSM-CERES-Maize (dashed lines) and with CSM-IXIM (continuous lines).

of largest leaf) and LX (duration of the most long-lived leaf) (Fig. 9). Under favorable growing conditions, changing AX ± 30% resulted in a nearly proportional response in LAI (±25%); changing LX the same amount resulted in LAI changes of –7 to 3%. When the crop was growing under water and N limitations, however, LAI varied –40 to 20% in response to a ±30% change in LX; the response to variation in AX was considerably less (–11 to 7%). The AX parameter is linked to the calculation of leaf expansion and LX to the calculation of leaf senescence, two processes simulated separately by IXIM (Lizaso et al., 2003a). Under stress, leaf expansion is reduced while leaf senescence is accelerated, thus a change in AX would have less impact on LAI at silking than would a similar change in LX.

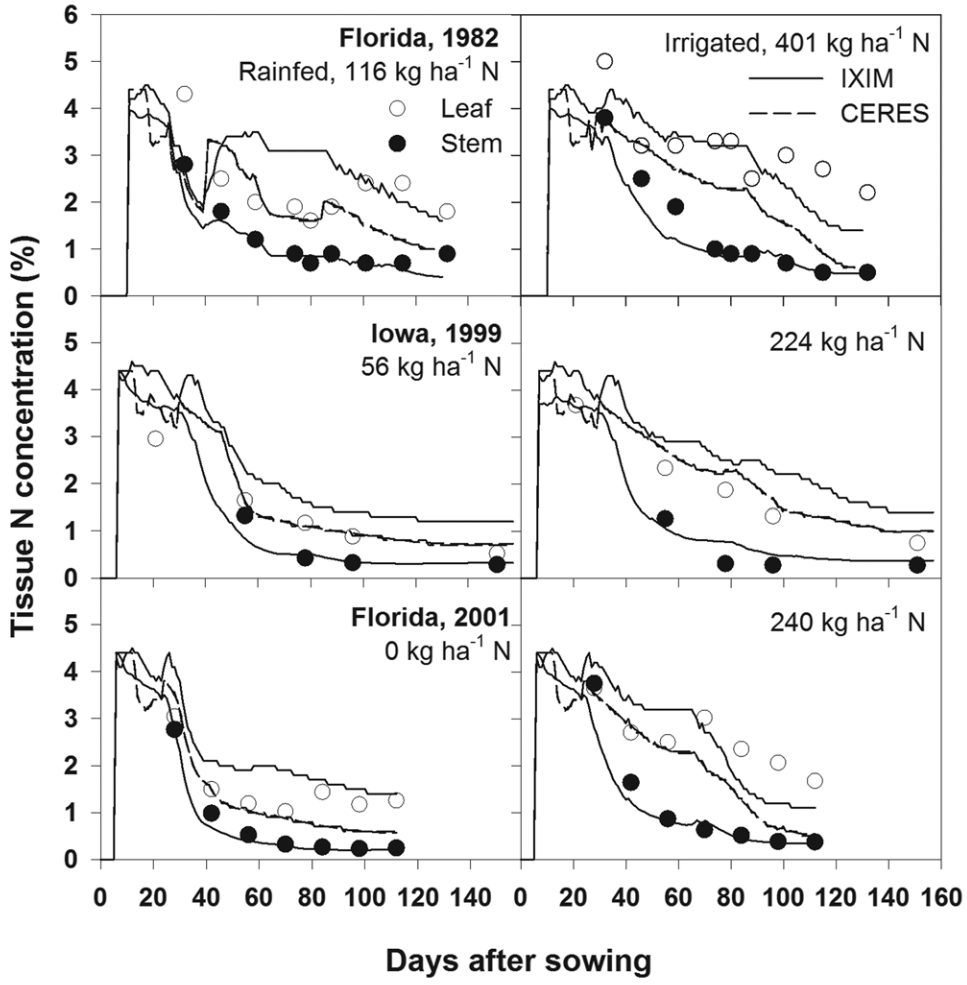

Fig. 8. Measured (symbols) and simulated (lines) N concentrations in leaves and stems of maize experiments conducted in Florida and Iowa. Simulations were obtained with CSM-CERES-Maize (dashed lines) and with CSM-IXIM (continuous lines); CSM-CERES-Maize simulated identical concentrations in leaves and stems.

The P1 parameter controls the duration of the juvenile phase. In the absence of stress, increasing the duration of the juvenile phase resulted in more leaves differentiated and therefore greater LAI at silking. When the supply of water or N was limited, however, increasing the duration of the juvenile phase allowed water and N stress to develop further, resulting in decreased LAI at silking. This simulated result agrees with the common observation that short-season cultivars typically perform better in drought or N-limited environments.

The PHINT parameter (thermal time between two consecutive leaves) controls the velocity of leaf differentiation and leaf number. Smaller PHINT values resulted in faster leaf differentiation and a greater number of leaves at silking. Each additional leaf had a larger relative response for the lower LAI produced under stress compared with the higher LAI produced under no stress.

The biomass at maturity proved to be the most conservative variable among those examined. Relative changes in coefficients shown in Fig. 9 had effects on biomass partitioning among plant tissues (data not shown) but had little impact (less than ±1%) on the total biomass accumulated at maturity.

Changing the fraction of biomass partitioned to the ear (P_E, Eq. [10]) had minimum results (less than ±3%) on grain yield simulated by IXIM, where kernel set is not linked to ear growth but to shoot growth (Eq. [11]). Uncertainty associated with the simulation of ear growth was larger than the uncertainty associated with the calculation of shoot growth. For that reason, kernel number simulations were more robust when calculated as a function of shoot growth rate compared with simulations obtained as a function of ear growth rate. Grain yield was far more responsive to changes in the genetic coefficients G2 (potential kernel number) or G3 (potential kernel growth rate). Under stress-free conditions, lowering G2 or G3 by 30% decreased the grain yield by as much as 20%. In contrast, increasing these values by 30% resulted in only minimal gains in grain yield (<1%). Interestingly, the same increase in G2 or G3 improved the grain yield by 24% under stress conditions (Fig. 9, right panel). In this example, plants were grown in sandy soil. Simulations indicated that little N was available within the root zone of unstressed plants by the end of the season. The combined effect of heavy crop N extraction and abundant irrigation resulted in plants growing under increasing N stress during the second half of the grain-filling phase. As such, grain growth depended mostly on remobilization of existing dry mass and no yield response was simulated after 30% increase in sink size (G2) or sink activity (G3). Under stress conditions, on the other hand, more N remained available within the root zone during grain filling, making grain yield more responsive to increments in either G2 or G3.

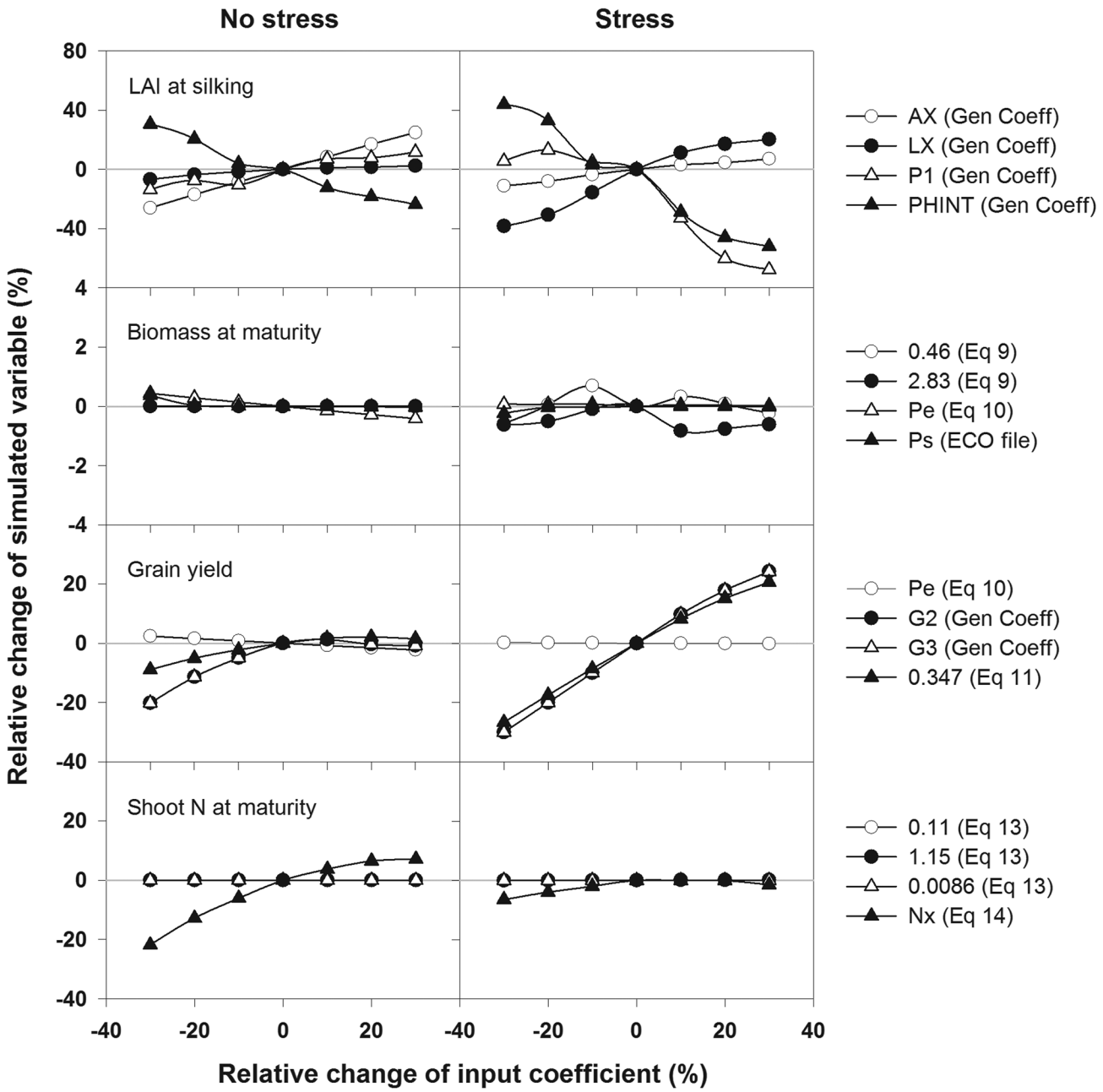

Fig. 9. Sensitivity analysis of CSM-IXIM performed by changing one parameter each time within ±30% for treatments without and with stress. The stress treatment received 5% of the seasonal irrigation and 29% of the N fertilization of the no-stress treatment, thus growing under stress most of the season. Parameters were directly associated with the simulation of leaf area index (LAI) at silking and biomass accumulation, grain yield, and N content at maturity. The parameters considered included one-side surface area of the largest leaf (AX), longevity of the longest lived leaf (LX), thermal time from emergence to the end of the juvenile phase (P1), thermal time elapsed between emergence of two consecutive leaf tips (PHINT), fraction of assimilates partitioned to the ear (P_E) and the stem (P_S), potential kernel number (G2), potential kernel growth rate (G3), and maximum N uptake rate under unrestricted conditions (NX); Gen. Coeff. = genetic coefficient.

Similar to changes in G2 and G3 were the effects of changing the efficiency of kernel set (slope in Eq. [11]). Increasing the slope in Eq. [11] would result in greater kernel set at a given plant growth rate, thus the response is similar to changing G2.

The stability of crop N acquisition was tested by changing the parameters associated with the calculation of critical N concentrations, target levels to compute daily N demand, of leaves, stems, and ears (Eq. [13]). These changes had always negligible effects on seasonal N content in the aboveground crop tissues. Changing the value of parameter Nx (maximum daily plant N uptake, Eq. [14]), however, had significant effects on the seasonal N uptake, especially under favorable growing conditions. Equation [14] was introduced in IXIM to limit the excessive N uptake simulated by CERES when soil N becomes highly available, especially following fertilization. Clearly, when Nx is reduced, Eq. [14] simulates more restriction to N uptake and thus a larger relative change than increasing Nx and making N uptake less restrictive.

CONCLUSIONS

We developed a new maize simulation model, IXIM, fully compatible with DSSAT standards as an alternative to the widely used CERES. The IXIM model offers a modular platform to continue developing and testing model improvements while maintaining availability of the well-established legacy of CERES. Both models are available in DSSAT version 4.5. The IXIM model requires two additional genetic coefficients, allowing cultivar-specific simulations of leaf area. When these coefficients are not available, the model calculates default values. New coefficients, defined in Table 1, are available to users in the ecotype and species files. The new model uses the same soil inputs and minimum weather data set (solar radiation, maximum and minimum temperatures, and rainfall) as CERES.

The IXIM model accurately simulated leaf area, biomass, grain yield, and crop N dynamics for a fairly wide range of treatments tested in this study. The new simulation of leaf area provided the flexibility to accommodate specific cultivars with various patterns of leaf expansion and senescence. Total aboveground biomass and grain yield were accurately simulated by both models; however, CERES tended to overestimate leaf growth and underestimate stem growth. On the other hand, IXIM simulated leaf mass close to measured values under most conditions but overestimated stem growth, particularly after recovery from water stress. Even though both models adequately calculated the total crop N acquisition, N uptake by CERES was too rapid after fertilization events. We showed that the CERES N partitioning between stems and leaves produced inaccurate results. On the contrary, IXIM produced excellent simulated results for stem N concentrations. Simulation of leaf N concentrations requires further refinements.

The IXIM model did show the expected response to changes in selected input parameters. Leaf area was highly responsive to changes in the new genetic coefficients AX and LX, and to changes in P1 and PHINT for their effect on leaf number. Total accumulation of biomass at maturity showed only minor variation when coefficients related to biomass partitioning were changed. Grain yield, in contrast, was very sensitive to changes in the genetic coefficients G2 and G3 and to changes in the efficiency of kernel set (Eq. [11]). Only the coefficient Nx, the maximum daily N uptake in Eq. [14], had a significant effect on the seasonal N accumulation in shoots.

In summary, the additional model equations and new algorithms incorporated into the modular maize model IXIM provide a stable and accurate simulation tool for current use and to continue future model development.

ACKNOWLEDGMENTS

This work was partially supported by the Regional Autonomous Government of Madrid (CM) and Polytechnic University of Madrid (UPM) under Cooperative Agreement CCG10-UPM/AGR-5789.

REFERENCES

Anapalli, S.S., L. Ma, D.C. Nielsen, M.F. Vigil, and L.R. Ahuja. 2005. Simulating planting date effects on corn production using RZWQM and CERES-Maize models. Agron. J. 97:58–71.

Andrade, F.H., C. Vega, S. Uhart, A. Cirilo, M. Cantarero, and O. Valentinuz. 1999. Kernel number determination in maize. Crop Sci. 39:453–459.

Asadi, M.E., and R.S. Clemente. 2001. Simulation of maize yield and N uptake under tropical conditions with the CERES-Maize model. Trop. Agric. 78:211–217.

Ben Nouna, B., N. Katerji, and M. Mastrorilli. 2000. Using the CERES-Maize model in a semi-arid Mediterranean environment: Evaluation of model performance. Eur. J. Agron. 13:309–322.

Birch, C.J., G.L. Hammer, and K.G. Rickert. 1998. Improved methods for predicting individual leaf area and leaf senescence in maize (*Zea mays*). Aust. J. Agric. Res. 49:249–262.

Birch, C.J., J. Vos, and P.E.L. van der Putten. 2003. Plant development and leaf area production in contrasting cultivars of maize grown in a cool temperate environment in the field. Eur. J. Agron. 19:173–188.

Boote, K.J., and N.B. Pickering. 1994. Modeling photosynthesis of row crop canopies. HortScience 29:1423–1434.

Carberry, P.S., R.C. Muchow, and R.L. McCown. 1989. Testing the CERES-Maize simulation model in a semi-arid tropical environment. Field Crops Res. 20:297–315.

Carlesso, R. 1993. Influence of soil water deficits on maize growth and leaf area adjustments. Ph.D. diss. Michigan State Univ., East Lansing (Diss. Abstr. 9406468).

Choudhury, B.J. 2001. Modeling radiation- and carbon-use efficiencies of maize, sorghum, and rice. Agric. For. Meteorol. 106:317–330.

Dwyer, L.M., D.W. Steward, R.I. Hamilton, and L. Houwing. 1992. Ear position and vertical distribution of leaf area in corn. Agron. J. 84:430–438.

Echarte, L., F.H. Andrade, C.R.C. Vega, and M. Tollenaar. 2004. Kernel number determination in Argentinean maize hybrids released between 1965 and 1993. Crop Sci. 44:1654–1661.

Elings, A. 2000. Estimation of leaf area in tropical maize. Agron. J. 92:436–444.

Gabrielle, B., S. Menasseri, and S. Houot. 1995. Analysis and field evaluation of the Ceres models water balance component. Soil Sci. Soc. Am. J. 59:1403–1412.

Godwin, D.C., and C.A. Jones. 1991. Nitrogen dynamics in the soil–plant systems. p. 289–321. *In* J. Hanks and J.T. Ritchie (ed.) Modeling plant and soil systems. Agron. Monogr. 31. ASA, CSSA, and SSSA, Madison, WI.

Goudriaan, J. 1977. Crop micrometeorology: A simulation study. Pudoc, Wageningen, the Netherlands.

Grant, R.F. 1989. Simulation of carbon assimilation and partitioning in maize. Agron. J. 81:563–571.

Hoogenboom, G., C.H. Porter, P.W. Wilkens, K.J. Boote, L.A. Hunt, J.W. Jones, et al. 2010. The Decision Support System for Agrotechnology Transfer (DSSAT): Past, current and future developments. p. 50–51. *In* Program and Summaries, Biological Systems Simulation Conf., 40th, Maricopa, AZ. 13–15 Apr. 2010. USDA-ARS Arid-Land Agric. Res. Ctr., Maricopa, AZ.

IBSNAT. 1989. Decision Support System for Agrotechnology Transfer, version 2.1: User guide. Dep. of Agron. and Soil Sci., College of Trop. Agric. and Human Resour., Univ. of Hawaii, Honolulu.

Jones, C.A. 1983. A survey of the variability in tissue nitrogen and phosphorus concentrations in maize and grain sorghum. Field Crops Res. 6:133–147.

Jones, C.A., and J.R. Kiniry. 1986. CERES-Maize: A simulation model of maize growth and development. Texas A&M Univ. Press, College Station.

Jones, J.W., G. Hoogenboom, C.H. Porter, K.J. Boote, W.D. Batchelor, L.A. Hunt, P.W. Wilkens, U. Singh, A.J. Gijsman, and J.T. Ritchie. 2003. The DSSAT cropping system model. Eur. J. Agron. 18:235–265.

Keating, B.A., and B.M. Wafula. 1992. Modeling the fully expanded area of maize leaves. Field Crops Res. 29:163–176.

Keeling, C.D., S.C. Piper, R.B. Bacastow, M. Wahlen, T.P. Whorf, M. Heimann, and H.A. Meijer. 2001. Exchanges of atmospheric CO_2 and $^{13}CO_2$ with the terrestrial biosphere and oceans from 1978 to 2000: I. Global aspects. SIO Ref. Ser. 01-06. Scripps Inst. of Oceanogr., San Diego.

Lindquist, J.L., and D.A. Mortensen. 1999. Ecophysiological characteristics of four maize hybrids and *Abutilon theophrasti*. Weed Res. 39:271–285.

Lizaso, J.I., W.D. Batchelor, K.J. Boote, and M.E. Westgate. 2005a. Development of a leaf-level canopy assimilation model for CERES-Maize. Agron. J. 97:722–733.

Lizaso, J.I., W.D. Batchelor, K.J. Boote, M.E. Westgate, P. Rochette, and A. Moreno-Sotomayor. 2005b. Evaluating a leaf level canopy assimilation model in CERES-Maize. Agron. J. 97:734–740.

Lizaso, J.I., W.D. Batchelor, and M.E. Westgate. 2003a. A leaf area model to simulate cultivar-specific expansion and senescence of maize leaves. Field Crops Res. 80:1–17.

Lizaso, J.I., W.D. Batchelor, M.E. Westgate, and L. Echarte. 2003b. Enhancing the ability of CERES-Maize to compute light capture. Agric. Syst. 76:293–311.

Lizaso, J.I., K.J. Boote, C.M. Cherr, J.M.S. Scholberg, J.J. Casanova, J. Judge, J.W. Jones, and G. Hoogenboom. 2007. Developing a sweet corn simula-

tion model to predict fresh market yield and quality of ears. J. Am. Soc. Hortic. Sci. 132:415–422.

Lizaso, J.I., and J.T. Ritchie. 1997. A modified version of CERES to predict the impact of soil water excess on maize crop growth and development. p. 153–167. *In* M.J. Kropff et al. (ed.). Applications of systems approaches at the field level. Vol. 2. Kluwer Acad. Publ., London.

Lopez-Cedron, F.X., K.J. Boote, B. Ruiz-Nogueira, and F. Sau. 2005. Testing CERES-Maize versions to estimate maize production in a cool environment. Eur. J. Agron. 23:89–102.

Mastrorilli, M., N. Katerji, and B. Ben Nouna. 2003. Using the CERES-Maize model in a semi-arid Mediterranean environment: Validation of three revised versions. Eur. J. Agron. 19:125–134.

Naidu, S.L., S.P. Moose, A.K. Al-Shoaibi, C.A. Raines, and S.P. Long. 2003. Cold tolerance of C4 photosynthesis in *Miscanthus* × *giganteus*: Adaptation in amounts and sequence of C4 photosynthetic enzymes. Plant Physiol. 132:1688–1697.

Nelder, J.A. 1962. New kinds of synthetic designs for spacing experiments. Biometrics 18:283–307.

Oberhuber, W., and G.E. Edwards. 1993. Temperature dependence of the linkage of quantum yield of photosystem II to CO_2 fixation in C4 and C3 plants. Plant Physiol. 101:507–512.

Otegui, M.E., and R. Bonhomme. 1998. Grain yield components in maize: I. Ear growth and kernel set. Field Crops Res. 56:247–256.

Pagano, E., and G.A. Maddonni. 2007. Intra-specific competition in maize: Early established hierarchies differ in plant growth and biomass partitioning to the ear around silking. Field Crops Res. 101:306–320.

Pang, X.P., J. Letey, and L. Wu. 1997. Yield and nitrogen uptake prediction by CERES-Maize model under semiarid conditions. Soil Sci. Soc. Am. J. 61:254–256.

Penning de Vries, F.W.T., and H.H. van Laar (ed.). 1982. Simulation of plant growth and crop production. Pudoc, Wageningen, the Netherlands.

Priestley, C.H.B., and R.J. Taylor. 1972. On the assessment of surface heat flux and evaporation using large-scale parameters. Mon. Weather Rev. 100:81–92.

Salah, H.B.H., and F. Tardieu. 1996. Quantitative analysis of the combined effects of temperature, evaporative demand and light on leaf elongation rate in well-watered field and laboratory-grown maize plants. J. Exp. Bot. 47:1689–1698.

Sonohat, G. 1997. Analyse des variations de structure aerienne de peuplements de maïs dans differentes conditions de competition intraspecifique. Ph.D. diss. Univ. de Paris, Orsay, France.

Spitters, C.J.T., H.A.J.M. Toussaint, and J. Goudriaan. 1986. Separating the diffuse and direct component of global radiation and its implications for modeling canopy photosynthesis: I. Components of incoming radiation. Agric. For. Meteorol. 38:217–229.

Stirling, C.M., C. Aguilera, N.R. Baker, and S.P. Long. 1994. Changes in the photosynthetic light response curve during leaf development of field grown maize with implications for modeling canopy photosynthesis. Photosynth. Res. 42:217–225.

Suleiman, A.A., and J.T. Ritchie. 2003. Modeling soil water redistribution during second stage evaporation. Soil Sci. Soc. Am. J. 67:377–386.

Tanaka, A., and J. Yamaguchi. 1972. Dry matter production, yield components and grain yield of the maize plant. J. Fac. Agric. Hokkaido Univ. 57:71–132.

Thiagarajah, M.R., and L.A. Hunt. 1982. Effects of temperature on leaf growth in corn (*Zea mays*). Can. J. Bot. 60:1647–1652.

Thornley, J.H.M., and I.R. Johnson. 1990. Plant and crop modeling: A mathematical approach to plant and crop physiology. Clarendon Press, Oxford, UK.

Tojo-Soler, C.M., P.U. Sentelhas, and G. Hoogenboom. 2007. Application of the CSM-CERES-maize model for planting date evaluation and yield forecasting for maize grown off-season in a subtropical environment. Eur. J. Agron. 27:165–177.

Warrington, I.J., and R.A. Norton. 1991. An evaluation of plant growth and development under various daily quantum integrals. J. Am. Soc. Hortic. Sci. 116:544–551.

Wilkerson, G.G., J.W. Jones, K.J. Boote, K.T. Ingram, and J.W. Mishoe. 1983. Modeling soybean growth for crop management. Trans. ASAE 26:63–73.

Willmott, C.J. 1982. Some comments on the evaluation of model performance. Bull. Am. Meteorol. Soc. 63:1309–1313.

Yang, H.S., A. Dobermann, J.L. Lindquist, D.T. Walters, T.J. Arkebauer, and K.G. Cassman. 2004. Hybrid-maize: A maize simulation model that combines two crop modeling approaches. Field Crops Res. 87:131–154.